HINGELESS ROTOR THEORY AND EXPERIMENT ON VIBRATION REDUCTION BY PERIODIC VARIATION OF CONVENTIONAL CONTROLS

G. J. Sissingh and R. E. Donham
Lockheed-California Company
Burbank, California

Abstract

The reduction of the n per rev. pitch-, roll- and vertical vibrations of an n-bladed rotor by n per rev. sinusoidal variations of the collective and cyclic controls is investigated. The numerical results presented refer to a four-bladed, 7.5-foot model and are based on frequency response tests conducted under an Army-sponsored research program. The following subjects are treated:

- Extraction of the rotor transfer functions (.073R hub flapping and model thrust versus servo valve command, amplitude and phase)
- Calculation of servo commands (volts) required to compensate .073R hub flapping (3P and 5P) and model thrust (4P)
- Evaluation of the effect of the vibratory control inputs on blade loads
- Theoretical prediction of the root flapbending moments generated by o to 5P perturbations of the feathering angle and rotor angle of attack.

Five operating conditions are investigated covering advance ratios from approximately 0.2 to 0.85. The feasibility of vibration reduction by periodic variation on conventional controls is evaluated.

Summary

For several operating conditions covering advance ratios from approximately 0.2 to 0.85, the control inputs required to counteract the existing 4P pitch, roll and vertical vibrations are calculated. The investigations are based on experimental vibration and response data. As the tests were part of and added on to a larger hingeless rotor research program, only a few operating conditions with essentially zero tip path plane tilt were investigated because of limited tunnel time. At the test rotor speed (500 rpm) the rotor blade mode frequencies were 1.34P, first flapping, 6.3P, second flapping, and 3.6P, first inplane.

This work was conducted under the sponsorship of the Ames Directorate of the U. S. Army Air Mobility R&D Laboratory under Contract NAS2-7245. The authors gratefully acknowledge the assistance of Mr. David Sharpe, the AMRDL Project Engineer, and Messrs. R. London and G. Watts of Lockheed in conducting the experimental portion of this work.

Presented at the AHS/NASA-Ames Specialists' Meeting on Rotorcraft Dynamics, February 13-15, 1974.

It should be noted that there was no instrumentation to measure the vibratory pitching and rolling moments. These moments were obtained by properly adding up the flap-bending moments of the four blades at 3.3 in. (0.073R) which were measured separately. This means, the effects of the inplane forces, vertical shear forces and blade torsion have been ignored. These are important influences in current hingeless rotor designs. The inplane 3P and 5P shear forces are of particular interest. However, the experimental data obtained for a model hingeless rotor system provides the beginning of at least a partial data base for the investigation of vibration attenuation of such systems through periodic variation of conventional controls.

Generally speaking, the control inputs required for flapping (hub moment) sourced vibration elimination are smaller or about of the same magnitude as those used for the frequency response tests. Their amplitudes lie, depending on flight condition and advance ratio, between 0.2 and 3 degrees. With the exception of the $\mu = 0.851$ case, for which the results are somewhat in doubt (the response tests to lateral cyclic pitch and the corresponding baseline data were inadvertently run with 0.3-degree collective pitch differential), the control inputs required for vibration reduction drastically reduce the 3 and 5P, and have only a minor effect on the 2P flexure flap-bending moments. Chord-bending moments and blade torsion generally increase.

The theoretical predictions mentioned refer to forced-response influence coefficients. They are based on the first two flapping modes. The blade root flap-bending moments (0P through 5P) which result from unit perturbations of blade feathering angle and rotor angle of attack have been calculated. The solution provides for intermode coupling through the 17th harmonic by analytic solution of the two-degree-of-freedom system, utilizing constant coefficient and loading descriptions over ten-degree azimuth sectors. In each solution case, the rotor reached steady-state motion in eight revolutions. In that time the least converging second mode flapping motion converged to a minimum of four significant figures.

Evaluation of the test data reveals two types of shortcomings, which should be avoided in future tests. First, the data given are based on a single test and have not been verified. Second, in some cases, the baseline and frequency response tests were not run successively.

From the data available, the approach is promising, especially for the low and medium advance ratio range. At higher advance ratios ($\mu \sim 0.8$), the control inputs required for vibration reduction may become prohibitive.

Notation

A, B — quantities describing cos 4ψ and sin 4ψ components of actuator input for frequency response tests, volt, see Table II and Equation (1)

C, D — quantities describing responses to A and B, in.-lb and lb, respectively, see Equation (1)

E, F, G, H — blade loads due to unit actuator input, in.-lb/ volt, see Equation (13)

$K_1 \ldots K_{18}$ — gains of rotor response, see Table I

m — calculated flapbending moment at 3.3 in., in.-lb,

$$m = m_o + \Sigma m_{ns} \sin n\psi + \Sigma m_{nc} \cos n\psi$$

M, L, T — 4P vibratory pitching moments, rolling moments and thrust variations, in.-lb and lb, respectively; subscript e denotes existing vibrations to be compensated, subscript control describes effects of oscillatory control inputs.

$$M_e = M_s \sin 4\psi + M_c \cos 4\psi$$

$$L_e = L_s \sin 4\psi + L_c \cos 4\psi$$

$$T_e = T_s \sin 4\psi + T_c \cos 4\psi$$

$\theta_{nominal}$ — nominal collective pitch, degrees

θ_o, θ_s, θ_c — oscillator inputs for collective, longitudinal and lateral cyclic pitch, volt

$$\theta_o = \theta_{os} \sin 4\psi + \theta_{oc} \cos 4\psi$$

$$\theta_s = \theta_{ss} \sin 4\psi + \theta_{sc} \cos 4\psi$$

$$\theta_c = \theta_{cs} \sin 4\psi + \theta_{cc} \cos 4\psi$$

$\tau_1 \ldots \tau_{18}$ — lag angles of response, degrees, see Table I

Ω — rotor angular velocity, $\sec^{-1}$

ψ — azimuth position of master blade, rad

$$\frac{C_{RM}}{a\sigma} = \frac{\text{Blade Root Moment, STA (o)}}{\pi R^3 \ \rho(\Omega R)^2 a\sigma}$$

where

$a = 5.73$

$\rho = 0.002378$ slugs/ft^3

$\sigma = 0.127$

"Compensating Control Inputs" define those which reduce the existing 4P pitching moments, rolling moments and vertical forces of a given flight condition to zero.

The analysis deals with the concept of vibration reduction by oscillatory collective and cyclic control applications. Several related aspects of this problem are treated. The foremost are the determination of the proper control inputs and their effect on the vibratory blade loads. These studies are based on frequency response tests conducted on a 7.5 foot-diameter, four-bladed, hingeless rotor model, the results of which are published in Appendixes C and D of Reference 1. The subject matter covered, apart from the items listed below, is an abridged version of these appendixes.

Other subjects treated are (a) the calculation of blade loads, based on test data, due to vibratory control command applications; (b) the theoretically determined eigenvalues, at 10-degree azimuth intervals, of the first and second flapping modes, at $\mu = 0.191$, 0.45 and 0.851; (c) the computed single-blade root flap-bending moment, Sta 0, harmonic influence coefficients at $\mu = 0.191$, 0.45 and 0.851; and (d) a limited comparison of the theoretical loads with experiments.

The general case of vibration control will include the effects of lateral and fore-and-aft shear forces at blade passage frequency. These forces can be as influential as the pitch and roll moment and thrust oscillations in causing fuselage vibrations. Thus, in general, five rotor vibratory inputs are to be controlled by manipulation of three controls. Although the five vibratory inputs cannot be nulled individually with three controls, their combined contribution to the fuselage vibration can be controlled. Thus, the general application will involve control of fuselage vibration at three points; say two vertical vibrations and one roll angular vibration. This general application implies the use of adaptive feedback controls. Although the present paper is limited to the more simple case outlined herein, the general application to the control of any three suitable quantities will be apparent.

Although prior investigations of the use of higher harmonic pitch control on teetering and offset hinge rotors have been conducted to investigate improved system performance and also for vibration attentuation (References 2, 3 and 4), this is believed to be the first experimental and theoretical hingeless rotor study of the use of periodic variation of conventional controls for vibration attentuation. The use of 2P feathering to improve rotor performance is not included as part of this work.

Transfer Functions Involved

As a distinction must be made between control applications in phase with sin 4ψ and cos 4ψ, there are six control quantities available, i.e., θ_{os}, θ_{oc}, θ_{ss}, θ_{sc}, θ_{cs} and θ_{cc}, to monitor the pitching moments, rolling moments and vertical forces. This means the dynamic system investigated, which consists of rotor, control mechanism and oscillators used, is characterized by 18 gains K_p and lag angles τ_p. The subscripts p (p = 1 through 18) are defined by Table I.

TABLE I
GAINS AND LAG ANGLES OF RESPONSE
TO OSCILLATORY CONTROL APPLICATIONS

	θ_{os}	θ_{oc}	θ_{ss}	θ_{sc}	θ_{cs}	θ_{cc}
M	$K_1 \tau_1$	$K_2 \tau_2$	$K_3 \tau_3$	$K_4 \tau_4$	$K_5 \tau_5$	$K_6 \tau_6$
L	$K_7 \tau_7$	$K_8 \tau_8$	$K_9 \tau_9$	$K_{10} \tau_{10}$	$K_{11} \tau_{11}$	$K_{12} \tau_{12}$
T	$K_{13} \tau_{13}$	$K_{14} \tau_{14}$	$K_{15} \tau_{15}$	$K_{16} \tau_{16}$	$K_{17} \tau_{17}$	$K_{18} \tau_{18}$

As indicated, K_3 is defined as the amplitude ratio M/θ_{ss} and τ_3 is the lag angle of M with respect to θ_{ss}. For convenience, the dimensions used are identical with those of the computer output, i.e., oscillator voltage for input, in.-lb for M and L, lb for the thrust variation T. This means the dimensions of K_p are

K_1 through K_{12}	in.-lb/volt
K_{13} through K_{18}	lb/volt

The phase angles τ_p are given in degrees, τ_p is positive if the response lags.

Although the investigations deal exclusively with 4P control variations, some general remarks may be in order. The general case involves sinusoidal collective and cyclic control variations with the frequency $n\Omega$ where n can be any positive number.

If n is an integer, the rotor excitations repeat themselves after each rotor revolution which means that the responses of each revolution are identical. This is true for any number of rotor blades but does not necessarily mean that all blades execute identical flapping motions. The latter is true only if n equals the number of rotor blades or is a multiple of the blade number. Only for these cases does a truly time independent response with invariable amplitude ratios K and lag angles τ exist.

Extraction of Gains and Lag Angles from Experiments

As for all response tests conducted, the oscillator input contained both sin 4ψ and cos 4ψ-components; always two amplitude ratios K and two lag angles τ are involved. Therefore, each time a set of two tests must be evaluated. According to Table II, the input is characterized by the quantities $A_1\ B_1\ A_2\ B_2$ and the response by $C_1\ D_1\ C_2\ D_2$.

If the rotor responds to cos 4ψ excitations with the gain K_j and the lag angle τ_j (j = even number) and to sin 4ψ excitations with K_i and τ_i (i = odd number), input and output are related by the equations

$$\left.\begin{aligned} A_1 K_j \cos(4\psi - \tau_j) + B_1 K_i \sin(4\psi - \tau_i) &= C_1 \cos 4\psi \\ &\quad + D_1 \sin 4\psi \\ A_2 K_j \cos(4\psi - \tau_j) + B_2 K_i \sin(4\psi - \tau_i) &= C_2 \cos 4\psi \\ &\quad + D_2 \sin 4\psi \end{aligned}\right\} \quad (1)$$

TABLE II
INPUT AND OUTPUT NOTATIONS

Test	Input	Response
#1	$A_1 \cos 4\psi + B_1 \sin 4\psi$	$C_1 \cos 4\psi + D_1 \sin 4\psi$
#2	$A_2 \cos 4\psi + B_2 \sin 4\psi$	$C_2 \cos 4\psi + D_2 \sin 4\psi$

To calculate the unknowns $K_i\ K_j\ \tau_i$ and τ_j, a component analysis is used. The gains $K_i\ K_j$ are expressed as

$$\left.\begin{aligned} K_i &= (R_i^2 + I_i^2)^{1/2} \\ K_j &= (R_j^2 + I_j^2)^{1/2} \end{aligned}\right\} \quad (2)$$

See also Figure 1 which shows the oscillatory pitching moments due to combined θ_{ss} and θ_{sc} control applications. The moments generated are presented by rotating vectors where cos 4ψ is positive to the right and sin 4ψ positive down. This means, the vector positions shown refer to $\psi = 0$. By definition, the quantities $R_{i,j}$ characterize the responses in phase with the excitation and $I_{i,j}$ those out of phase. The latter are positive if the response leads. As indicated, there are altogether four responses involved which are combined to the resultant M.

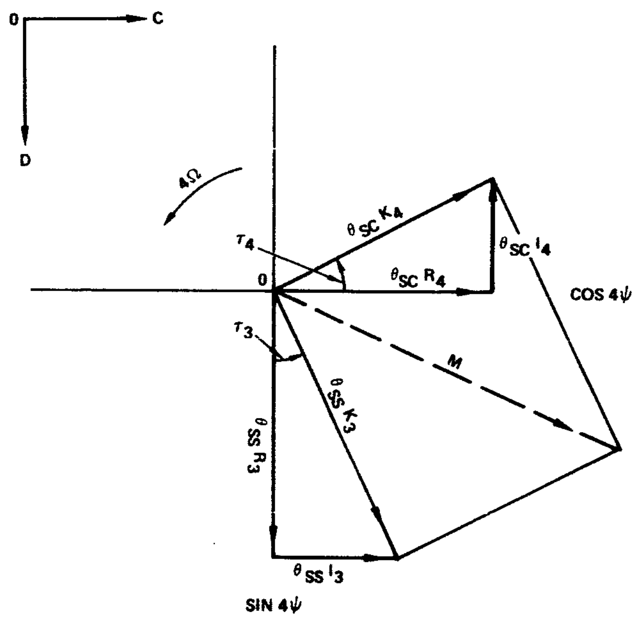

Figure 1. Vector Diagram Showing Pitching Moment Due to θ_{ss} and θ_{sc} Control Applications

Inserting Equation (2) into Equation (1) leads to

$$\left.\begin{aligned} R_i &= \frac{A_1 D_2 - A_2 D_1}{A_1 B_2 - A_2 B_1} \\ I_i &= \frac{A_1 C_2 - A_2 C_1}{A_1 B_2 - A_2 B_1} \\ \tan \overline{\tau}_i &= |I_i/R_i| \quad 0 < \overline{\tau}_i < \pi/2 \end{aligned}\right\} \quad (3)$$

and

$$\left.\begin{aligned} R_j &= \frac{C_1 B_2 - B_1 C_2}{A_1 B_2 - A_2 B_1} \\ I_j &= \frac{B_1 D_2 - B_2 D_1}{A_1 B_2 - A_2 B_1} \\ \tan \overline{\tau}_j &= |I_j/R_j| \quad 0 < \overline{\tau}_j < \pi/2 \end{aligned}\right\} \quad (4)$$

In both cases

$$
\begin{array}{llll}
\tau = +\bar{\tau} & \text{for} & R > 0 & I < 0 \\
 = -\bar{\tau} & & R > 0 & I > 0 \\
 = \pi + \bar{\tau} & & R < 0 & I > 0 \\
 = \pi - \bar{\tau} & & R < 0 & I < 0
\end{array}
$$

Check of Calculated K_i K_j τ_i and τ_j Values

If so desired, Equation (1) can be used to check the calculated values of K_i K_j τ_i and τ_j. Splitting up these equations into sin 4ψ and cos 4ψ components leads to the following four expressions which must be satisfied

$$
\left.
\begin{aligned}
A_1 K_j \cos\tau_j - B_1 K_i \sin\tau_i &= C_1 \\
A_1 K_j \sin\tau_j + B_1 K_i \cos\tau_i &= D_1 \\
A_2 K_j \cos\tau_j - B_2 K_i \sin\tau_i &= C_2 \\
A_2 K_j \sin\tau_j + B_2 K_i \cos\tau_i &= D_2
\end{aligned}
\right\} \qquad (5)
$$

Oscillatory Control Inputs Required

The six oscillator inputs available have to be selected so that their responses satisfy the requirements, whatever they may be. By definition, the vibratory control inputs result in the following pitching moments, rolling moments and vertical forces (n = 4):

$$
\begin{aligned}
M_{control} = &+\theta_{os} K_1 \sin(n\psi - \tau_1) \\
&+ \theta_{oc} K_2 \cos(n\psi - \tau_2) \\
&+ \theta_{ss} K_3 \sin(n\psi - \tau_3) \\
&+ \theta_{sc} K_4 \cos(n\psi - \tau_4) \\
&+ \theta_{cs} K_5 \sin(n\psi - \tau_5) \\
&+ \theta_{cc} K_6 \cos(n\psi - \tau_6)
\end{aligned}
\qquad (6)
$$

$$
\begin{aligned}
L_{control} = &+\theta_{os} K_7 \sin(n\psi - \tau_7) \\
&+ \theta_{oc} K_8 \cos(n\psi - \tau_8) \\
&+ \theta_{ss} K_9 \sin(n\psi - \tau_9) \\
&+ \theta_{sc} K_{10} \cos(n\psi - \tau_{10}) \\
&+ \theta_{cs} K_{11} \sin(n\psi - \tau_{11}) \\
&+ \theta_{cc} K_{12} \cos(n\psi - \tau_{12})
\end{aligned}
\qquad (7)
$$

$$
\begin{aligned}
T_{control} = &+\theta_{os} K_{13} \sin(n\psi - \tau_{13}) \\
&+ \theta_{oc} K_{14} \cos(n\psi - \tau_{14}) \\
&+ \theta_{ss} K_{15} \sin(n\psi - \tau_{15}) \\
&+ \theta_{sc} K_{16} \cos(n\psi - \tau_{16}) \\
&+ \theta_{cs} K_{17} \sin(n\psi - \tau_{17}) \\
&+ \theta_{cc} K_{18} \cos(n\psi - \tau_{18})
\end{aligned}
\qquad (8)
$$

$$
\left.
\begin{aligned}
M_{control} &= -M_s \sin 4\psi - M_c \cos 4\psi \\
L_{control} &= -L_s \sin 4\psi - L_c \cos 4\psi \\
T_{control} &= -T_s \sin 4\psi - T_c \cos 4\psi
\end{aligned}
\right\} \qquad (9)
$$

To reduce the existing vibrations, the moments and forces generated must counteract M_e, L_e and T_e, i.e.,

Equations 6 through 9 lead to six linear equations, (10), for the unknowns θ_{os}, θ_{oc}, θ_{ss}, θ_{sc}, θ_{cs} and θ_{cc}.

Effect on Blade Loads

An objective of the investigations is to determine the effect of the compensating control input on the blade loads, i.e., on the following measured quantities:

- flapbending at 3.3 in.
- flapbending at 13.15 in.
- chordbending at 2.4 in.
- torsion at 9.28 in.

In all cases the 2 to 5P content of the loads is of interest. The first task is to determine from the response tests the contribution of each of the six possible 4P control inputs to these loads. Again, two sets of data are required. The vibratory control applications used and the resulting n[th] harmonic of the load considered are written as follows:

Test	Input	Resulting Load (in.-lb)	
#1	$A_1 \cos 4\psi + B_1 \sin 4\psi$	$C_{n1} \cos n\psi + D_{n1} \sin n\psi$	(11)
#2	$A_2 \cos 4\psi + B_2 \sin 4\psi$	$C_{n2} \cos n\psi + D_{n2} \sin n\psi$	

$$
\begin{bmatrix}
+K_1\cos\tau_1 & +K_2\sin\tau_2 & +K_3\cos\tau_3 & +K_4\sin\tau_4 & +K_5\cos\tau_5 & +K_6\sin\tau_6 \\
-K_1\sin\tau_1 & +K_2\cos\tau_2 & -K_3\sin\tau_3 & +K_4\cos\tau_4 & -K_5\sin\tau_5 & +K_6\cos\tau_6 \\
+K_7\cos\tau_7 & +K_8\sin\tau_8 & +K_9\cos\tau_9 & +K_{10}\sin\tau_{10} & +K_{11}\cos\tau_{11} & +K_{12}\sin\tau_{12} \\
-K_7\sin\tau_7 & +K_8\cos\tau_8 & -K_9\sin\tau_9 & +K_{10}\cos\tau_{10} & -K_{11}\sin\tau_{11} & +K_{12}\cos\tau_{12} \\
+K_{13}\cos\tau_{13} & +K_{14}\sin\tau_{14} & +K_{15}\cos\tau_{15} & +K_{16}\sin\tau_{16} & +K_{17}\cos\tau_{17} & +K_{18}\sin\tau_{18} \\
-K_{13}\sin\tau_{13} & +K_{14}\cos\tau_{14} & -K_{15}\sin\tau_{15} & +K_{16}\cos\tau_{16} & -K_{17}\sin\tau_{17} & +K_{18}\cos\tau_{18}
\end{bmatrix}
\begin{bmatrix}
\theta_{os} \\ \theta_{oc} \\ \theta_{ss} \\ \theta_{sc} \\ \theta_{cs} \\ \theta_{cc}
\end{bmatrix}
=
\begin{bmatrix}
-M_s \\ -M_c \\ -L_s \\ -L_c \\ -T_s \\ -T_c
\end{bmatrix}
\qquad (10)
$$

If nonlinear effects are excluded, the n per rev load variation due to unit control application in phase with

$$\left.\begin{array}{lll} \text{(a)} & \cos 4\psi \text{ amounts to} & (E_n \cos n\psi + F_n \sin n\psi) \\ \text{(b)} & \sin 4\psi & (G_n \cos n\psi + H_n \sin n\psi) \end{array}\right\} \quad (12)$$

In these expressions

$$\left.\begin{aligned} E_n &= \frac{B_2C_{n1} - B_1C_{n2}}{A_1B_2 - A_2B_1} \\ F_n &= \frac{B_2D_{n1} - B_1D_{n2}}{A_1B_2 - A_2B_1} \\ G_n &= \frac{A_1C_{n2} - A_2C_{n1}}{A_1B_2 - A_2B_1} \\ H_n &= \frac{A_1D_{n2} - A_2D_{n1}}{A_1B_2 - A_2B_1} \end{aligned}\right\} \quad (13)$$

If $\theta_{\xi s}$, $\theta_{\xi c}$ (ξ = o, s, c) denote the vibratory control inputs used, the increments of the n^{th} harmonic of the load considered are

$$\begin{aligned} (\Delta\text{load})_n &= (\theta_{\xi c} E_n + \theta_{\xi s} G_n) \cos n\psi \\ &\quad + (\theta_{\xi c} F_n + \theta_{\xi s} H_n) \sin n\psi \end{aligned} \quad (14)$$

Evaluation of Experiments

Flight Conditions Investigated

The methods outlined in the previous sections are applied to the following five operating conditions for which test data are available:

TABLE III
OPERATING CONDITIONS INVESTIGATED

μ	$\theta_{nominal}$	α	C_T/σ
0.191	12°	-5°	0.102
0.239	4	-5	0.028
0.443	4	-5	0.011
0.849	10	-5	-0.005
0.851	4	-5	-0.013

In all cases the shaft angle of attack is $\alpha = -5^\circ$ and the rotor is trimmed so that essentially $a_1 = b_1 = 0$. As can be seen, the tests cover the advance ratio range from approximately $\mu = 0.2$ to $\mu = 0.85$. The case $\mu = 0.191$ is characterized by $\theta_{nominal} = 12^\circ$ and $C_T/\sigma = 0.102$, the latter figure indicates a relatively high specific loading. In contrast, at the advance ratios $\mu = 0.849$ and 0.851 the rotor is practically unloaded, i.e., no steady lifting force is generated. The 4P vibrations associated with the various test conditions are listed in Table IV. The moments are given in inch-pounds and the vibratory forces in pounds.

These moments were obtained by properly adding up the flap-bending moments of the four blades at 3.3 in. which were measured separately. This means, the effects of the in-plane forces, vertical shear forces and blade torsion have been ignored.

TABLE IV
VIBRATORY MOMENTS AND FORCES
TO BE COMPENSATED

μ	0.191	0.239	0.443	0.849	0.851
M_s	0.3805	- 1.7207	2.6149	20.0483	3.5349
M_c	- 0.5301	- 0.4113	- 0.5208	- 4.5724	- 8.4341
L_s	12.2080	1.3725	- 6.7626	9.4647	-10.5154
L_c	2.2180	- 1.9145	- 3.7399	- 31.1214	-17.2626
T_s	0.1979	- 0.1089	0.0304	1.9247	0.8838
T_c	- 0.2013	- 0.0865	0.0556	- 0.0048	- 0.8626

Gains and Lag Angles

The rotor response characteristics are calculated by applying equations (2, 3, 4) to the test data available. The results available are listed in Table V. As pointed out previously, the values given include the effect of the actuator used. Some general statements can be made. It is obvious that for $\mu = 0$. the gain and lag angle of the responses to sin 4ψ- and cos 4ψ-type control applications must be the same. For $\mu \neq 0$ this is no longer true, and one would expect that the spread between K_iK_j and $\tau_i\tau_j$ (see equations (3), (4)) widens with increasing advance ratio. Further, according to classical rotor theory which neglects blade stall, the nominal collective pitch setting has no effect on the frequency response characteristics.

Generally speaking, the K_iK_j and $\tau_i\tau_j$ values given in Table V differ very little. It appears however, that at higher advance ratios (compare columns for $\mu = 0.849$ and 0.851) the collective pitch has a larger effect than anticipated. It is also possible that the error of the baseline data described in the summary may play a role.

Oscillator Inputs Required

Equation (10) is used to calculate the inputs required to

(a) generate unit amplitudes of pure pitching moments, rolling moments and vertical forces and

(b) compensate the existing vibrations

The results are given in Tables VI and VII. They show that, as to be expected, the oscillatory inputs required for vibration reductions generally increase with increasing advance ratio. Surprisingly, the rotor collective pitch setting seems to play a larger role than the steady lift generated. See also Table VIII which summarizes the results obtained and lists the operating conditions investigated in the order of decreasing vibrations. The first column shows the relative magnitude of the vibratory moments generated and the last column the approximate amplitude of the blade pitch variation required to compensate the vibrations. The amplitude of the pitch variation produced per volt oscillator input changes with the control loads and

TABLE V
GAINS AND LAG ANGLES DERIVED FROM EXPERIMENTS
(K_p - in.-lb/volt, τ_p - degrees)

	μ = 0.191		μ = 0.239		μ = 0.443		μ = 0.849		μ = 0.851	
p	K_p	τ_p	K_p	τ_p	K_p	τ_p	K_p	τ_p	K_p	τ_p
1	5.617	42.3	1.099	125.6	2.236	120.5	4.798	72.0	4.094	116.5
2	6.126	44.0	1.141	149.1	2.791	129.3	4.787	72.6	3.487	135.6
3	17.571	-9.6	52.416	-30.1	42.237	-28.7	18.537	-19.8	43.319	-5.1
4	26.019	-45.4	47.991	-37.3	40.073	-30.1	20.329	-41.5	37.081	12.7
5	30.696	155.7	59.416	182.9	45.186	188.4	33.002	183.4	26.170	214.2
6	32.505	181.7	77.408	193.2	61.144	180.8	21.085	180.0	38.661	184.5
7	2.856	136.0	4.246	81.9	8.166	86.5	2.472	102.1	10.097	93.1
8	1.507	98.4	5.083	67.1	8.077	66.9	3.412	144.7	7.979	62.9
9	35.384	213.4	59.420	198.8	43.846	181.4	44.506	200.5	48.081	176.2
10	41.674	185.8	51.280	198.6	39.383	195.7	48.473	201.0	40.850	187.7
11	45.953	116.6	76.875	108.3	78.512	101.8	67.268	134.4	88.540	94.7
12	61.589	131.5	86.361	99.3	80.995	95.7	61.288	141.5	90.934	95.3
13	6.879	45.6	5.420	51.4	8.928	39.2	8.188	35.8	9.340	38.5
14	7.211	43.7	6.195	46.4	8.999	35.9	8.906	36.1	9.651	35.6
15	6.635	245.2	4.275	205.9	2.571	195.2	5.976	215.0	3.623	184.0
16	6.033	218.3	3.962	208.1	3.123	188.7	4.775	229.5	1.977	185.4
17	13.000	127.3	7.596	94.3	7.632	76.7	13.261	133.1	11.188	86.9
18	10.057	128.6	8.176	97.4	8.381	92.2	7.953	126.3	11.101	90.7

the type of control ($\theta_O, \theta_S, \theta_C$) used. Therefore, the conversion factor varies and the last column of Table VIII is given only to indicate the approximate amplitudes involved.

With one exception, the vibratory control applications required were smaller than those used for the frequency response tests. The exception is the case with the highest vibration level encountered for which the compensating controls required were approximately 15 to 20% higher than the inputs used for the 4P frequency response tests.

Blade Loads

The calculation of the effect of the compensating control inputs on the blade loads is based on Equations (13) and (14). The first step is to calculate, for each specific case, the quantities E_n through H_n (n = 2, 3, 4, 5). See Table IX which refers to μ = 0.849 and lists the sin $n\psi$ and cos $n\psi$ components of the various loads due to unit control (volt) application. The table shows, for instance, that at the advance ratio μ = 0.849, a ±1 volt variation of θ_{SS} produces 3P chordwise bending moments of the magnitude

$$(-91.77 \sin 3\psi + 7.15 \cos 3\psi) \text{ in.-lb}$$

As the control inputs required for vibration reduction have been previously calculated, their effects on the blade loads can be determined by adding up the various contributions. The reader is referred to Table X which applies to the flapbending moment at 3.3 in.for the case μ = 0.849. Given are the original loads without vibratory control application, the individual contributions and the sum. The last column shows the amplitudes without and with compensating control input. A summary of the loads is represented in Table XI. Generally speaking, chord-bending, blade torsion and the 4P flap-bending moments of the root flexure increase with increasing advance ratio. The 3 and 5P flap-bending moments of the flexure are, by nature, reduced and the 2P flap-bending moments are least affected. From the limited data available, it appears that the 4P chordwise- and 5P torsion moments may be the critical load for this configuration, inasmuch as the natural frequencies are close to these values.

As mentioned previously, it is assumed here that the pitching and rolling moments are solely caused by the flap-bending moments of the root flexure which were individually measured and properly combined by a sin-cos potentiometer. This means, the only source for the troublesome 4P moments in the nonrotating system are the 3 and 5P flap-bending moments at 3.3 in. For four identical blades, it follows that elimination of the 4P pitching and rolling moments requires that the sin 3ψ, cos 3ψ, sin 5ψ and cos 5ψ components of the flap-bending moments at 3.3 in. are reduced to zero. As the four blades behave differently, this ideal condition will practically never be fulfilled.

In the preceding paragraphs the flapbending moment of a specific blade, with consideration of the compensating control input, was calculated. To a certain extent, these predicted loads can be used as an independent check. As an example, the case μ = 0.849 is treated. According to Table IV the amplitudes of the 4P pitching and rolling moments to be compensated are

$$\begin{aligned} M &= 20.56 \text{ in.-lb} \\ L &= 32.52 \text{ in.-lb} \end{aligned} \qquad (15)$$

The calculated 3 and 5P flap-bending moments with consideration of the compensating control input amount to (see Table VII),

$$\begin{aligned} m_{3s} &= 0.6233 \text{ in.-lb} \\ m_{3c} &= -1.1833 \\ m_{5s} &= -1.9266 \\ m_{5c} &= 0.3099 \end{aligned} \tag{16}$$

The amplitudes of the resulting 4P pitching and rolling moments are

$$\begin{aligned} M &= 3.14 \text{ in.-lb} \\ L &= 5.91 \text{ in.-lb} \end{aligned} \tag{17}$$

TABLE VI
OSCILLATOR INPUTS REQUIRED (VOLT) TO GENERATE PURE sin 4ψ AND cos 4ψ COMPONENTS OF PITCHING MOMENTS, ROLLING MOMENTS AND VERTICAL FORCES

μ	$M_{control}$ *	θ_{os}	θ_{oc}	θ_{ss}	θ_{sc}	θ_{cs}	θ_{cc}
0.191	$M_{s,\,control} = 1$	+0.0143	-0.0485	+0.0508	+0.0290	-0.0296	+0.0241
	$M_{c,\,control} = 1$	+0.0117	-0.0123	-0.0055	+0.0283	-0.0219	-0.0098
	$L_{s,\,control} = 1$	-0.0177	-0.0236	-0.0113	+0.0052	-0.0169	+0.0073
	$L_{c,\,control} = 1$	+0.0042	-0.0071	-0.0209	-0.0200	+0.0003	-0.0147
	$T_{s,\,control} = 1$	+0.0922	+0.1380	-0.0490	-0.0302	+0.0252	-0.0232
	$T_{c,\,control} = 1$	-0.1044	+0.1164	+0.0123	-0.0210	+0.0235	+0.0081
0.239	$M_{s,\,control} = 1$	+0.0028	-0.0069	+0.0299	+0.0219	-0.0111	+0.0211
	$M_{c,\,control} = 1$	+0.0109	+0.0028	-0.0096	+0.0206	-0.0154	-0.0070
	$L_{s,\,control} = 1$	-0.0023	-0.0108	-0.0056	+0.0203	-0.0167	+0.0078
	$L_{c,\,control} = 1$	+0.0128	-0.0029	-0.0245	-0.0243	-0.0008	-0.0210
	$T_{s,\,control} = 1$	+0.1356	+0.1337	-0.0053	-0.0155	+0.0072	-0.0128
	$T_{c,\,control} = 1$	-0.1436	+0.1085	+0.0168	+0.0070	+0.0091	+0.0100
0.443	$M_{s,\,control} = 1$	-0.0019	-0.0053	+0.0255	+0.0116	-0.0069	+0.0145
	$M_{c,\,control} = 1$	+0.0053	+0.0011	-0.0023	+0.0331	-0.0168	-0.0004
	$L_{s,\,control} = 1$	-0.0057	-0.0067	-0.0021	+0.0253	-0.0135	+0.0126
	$L_{c,\,control} = 1$	+0.0120	-0.0028	-0.0155	-0.0084	-0.0093	-0.0112
	$T_{s,\,control} = 1$	+0.1020	+0.0732	-0.0088	-0.0094	-0.0018	-0.0138
	$T_{c,\,control} = 1$	-0.0714	+0.0941	+0.0071	-0.0108	+0.0171	-0.0024
0.849	$M_{s,\,control} = 1$	+0.0049	-0.0240	+0.0338	+0.0179	-0.0229	+0.0182
	$M_{c,\,control} = 1$	+0.0149	-0.0149	-0.0109	+0.0487	-0.0271	-0.0222
	$L_{s,\,control} = 1$	-0.0124	-0.0137	-0.0120	+0.0074	-0.0118	+0.0024
	$L_{c,\,control} = 1$	+0.0052	-0.0056	-0.0072	-0.0121	+0.0006	-0.0123
	$T_{s,\,control} = 1$	+0.1050	+0.0698	-0.0211	+0.0037	+0.0017	-0.0214
	$T_{c,\,control} = 1$	-0.0772	+0.1079	-0.0034	-0.0305	+0.0221	+0.0031
0.851	$M_{s,\,control} = 1$	+0.0001	-0.0081	+0.0191	+0.0122	-0.0077	+0.0109
	$M_{c,\,control} = 1$	+0.0082	-0.0055	-0.0126	+0.0290	-0.0135	-0.0055
	$L_{s,\,control} = 1$	-0.0080	-0.0107	-0.0043	+0.0117	-0.0057	+0.0098
	$L_{c,\,control} = 1$	+0.0113	-0.0102	-0.0069	+0.0028	-0.0137	-0.0037
	$T_{s,\,control} = 1$	+0.1016	+0.0599	-0.0087	+0.0109	-0.0130	-0.0091
	$T_{c,\,control} = 1$	-0.0682	+0.0998	+0.0034	-0.0143	+0.0189	-0.0058

* in.-lb

TABLE VII
OSCILLATOR INPUTS REQUIRED (VOLT)
TO COMPENSATE EXISTING 4P- VIBRATIONS

μ	0.191	0.239	0.443	0.849	0.851
θ_{os}	0.1683	0.0394	0.0146	0.0457	0.0300
θ_{oc}	0.3121	0.0224	-0.0490	0.2354	-0.2726
θ_{ss}	0.1746	0.0090	-0.1400	-0.7980	-0.3275
θ_{sc}	-0.0133	-0.0293	0.1273	-0.5881	0.3498
θ_{cs}	0.2052	-0.0026	-0.1176	0.4610	-0.3549
θ_{cc}	-0.0651	-0.0180	0.0056	-0.8308	-0.0428

TABLE VIII
VIBRATION SUMMARY

Rel. Vibration Level	μ	$\theta_{nominal}$	C_T/σ	Ampl. of Pitch Variation
1	0.849	10^o	-0.005	$\sim 3.0^o$
0.58	0.851	4	-0.013	2.0
0.32	0.191	12	0.102	0.8
0.21	0.443	4	0.011	0.5
0.08	0.239	4	0.028	0.2

Decreasing Vibration Level

TABLE IX
EFFECTS OF UNIT 4P OSCILLATOR INPUT ON BLADE BENDING
AND TORSION MOMENTS (in-lb). $\mu = 0.849$

$\mu = 0.849$	Input	sin 2ψ	cos 2ψ	sin 3ψ	cos 3ψ	sin 4ψ	cos 4ψ	sin 5ψ	cos 5ψ
Flapbending 3.3 in.	θ_{os}	0.3815	- 2.6028	- 1.1212	+ 1.9467	+ 0.0022	1.6252	- 0.4640	+ 0.2286
	θ_{oc}	- 0.7265	- 0.7428	- 2.1170	- 0.9082	- 1.7646	0.1744	+ 0.4336	- 0.2014
	θ_{ss}	- 20.1796	- 7.1252	0.4843	10.9746	9.2290	- 1.4705	- 12.1221	- 16.4408
	θ_{sc}	1.4455	- 18.6069	- 11.8793	0.8771	1.9670	9.2946	+18.4710	- 13.1116
	θ_{cs}	- 15.0717	19.2091	- 1.7568	+ 13.3006	4.4390	13.0827	24.2022	- 18.4700
	θ_{cc}	- 11.0041	- 12.5052	- 12.2451	- 3.9250	- 11.5818	6.8481	17.1269	+18.2863
Flapbending 13.15 in.	θ_{os}	- 3.1446	0.01156	+ 0.0644	- 6.4289	0.5673	- 5.5966	- 2.6912	- 5.2806
	θ_{oc}	0.4488	- 3.3139	+ 5.7587	- 0.6033	7.2213	1.7289	4.4109	- 1.9638
	θ_{ss}	- 13.1131	- 1.6401	- 9.4439	11.4718	2.7493	1.6368	20.3552	30.4485
	θ_{sc}	- 3.1093	- 10.4663	- 13.7168	- 7.3647	- 0.7250	4.6008	- 31.6355	23.4534
	θ_{cs}	- 15.3541	3.9011	- 20.8842	- 14.1583	- 4.0272	- 4.6816	- 53.1766	36.9531
	θ_{cc}	- 3.7738	- 10.2279	7.2742	- 11.8491	2.4534	1.0036	- 30.9619	- 33.3918
Chordbending 2.4 in.	θ_{os}	- 5.2318	5.1653	18.4997	- 66.4765	8.5046	- 2.0555	6.0027	8.6689
	θ_{oc}	- 0.3311	2.6008	55.9170	15.3823	8.5503	12.5308	- 10.1401	4.6381
	θ_{ss}	- 23.2604	3.6649	- 91.7693	7.1537	- 12.9172	- 5.1116	- 13.8450	7.4174
	θ_{sc}	4.7043	- 8.0015	- 37.9514	- 71.7419	6.5301	- 16.8130	- 4.2184	- 12.8505
	θ_{cs}	- 25.0714	15.3009	- 59.7492	- 177.5673	41.5059	- 80.7110	- 5.8153	- 27.4052
	θ_{cc}	- 2.0059	- 7.7253	77.1483	- 7.0902	68.5358	26.5134	7.7451	- 28.5566
Torsion 9.28 in.	θ_{os}	0.1891	0.0544	- 0.2460	0.5652	- 1.0733	0.2665	0.1925	0.0465
	θ_{oc}	0.0788	- 0.1531	- 0.1960	- 0.2328	- 0.6076	- 1.0110	0.0102	0.01822
	θ_{ss}	0.4975	0.2685	- 0.9271	- 1.5838	- 0.0498	1.4606	15.6374	13.1496
	θ_{sc}	- 0.6976	- 0.7498	3.0700	- 1.4345	- 1.0039	0.9952	- 11.8807	15.1709
	θ_{cs}	0.8756	- 0.0250	- 1.5421	- 0.9968	- 1.9762	1.0423	- 14.6088	21.3914
	θ_{cc}	- 0.8745	- 0.9375	2.1226	- 2.5792	- 1.3255	- 1.2713	- 17.9657	- 13.8937

Comparison of Equations (15) and (17) shows that the vibratory pitching moment is reduced to approximately 15 percent and the rolling moment to approximately 18 percent of its original value. This indicates that the various blades behave differently and that the goal of zero 4P pitch-roll and vertical vibrations is achieved by cancellation of the effects of the four blades.

Analytical Formulation and Calculated Results

The aeromechanical characteristics of the High Advance Ratio Model (HARM) has been analytically described in 2 degrees of freedom. These are based on the first and second flapping modes which have been approximated by polynomial fits of finite element determined mode shapes. The first and second mode shape approximations used are given by

$$\phi_1 = 2.292x^2 - 1.292x^3$$

and

$$\phi_2 = -10.21x^2 + 20.78x^3 - 9.57x^4$$

where

$x = \frac{r}{R}$; the non-dimensional radial station.

The aerodynamics are based on classical quasi-steady incompressible strip theory. The reverse flow region is fully accounted for, but stall effects have been neglected, as described in Reference 5.

TABLE X
EFFECT OF VIBRATION COMPENSATION ON FLAPBENDING MOMENT (in-lb) AT 3.3 in. $\mu = 0.849$

n		cos n	sin n	Amplitude
2	W/O Vibration Control	-92.7652	17.2338	94.35
	Contribution of θ_o	-0.0559	-0.1536	
	θ_s	16.6165	15.2507	
	θ_c	19.2393	2.2002	
	TOTAL	-56.9653	34.5311	66.61
3	W/O Vibration Control	-1.1732	-14.7883	14.83
	Contribution of θ_o	-0.1248	-0.5496	
	θ_s	-9.2715	6.5928	
	θ_c	9.3862	9.3684	
	TOTAL	-1.1833	0.6233	1.34
4	W/O Vibration Control	-0.1403	-3.5448	3.55
	Contribution of θ_o	0.1153	-0.4152	
	θ_s	-4.2868	-8.5191	
	θ_c	0.3317	11.6713	
	TOTAL	-3.9801	-0.8078	4.06
5	W/O Vibration Control	3.2312	2.2658	3.95
	Contribution of θ_s	-0.0370	0.0809	
	θ_s	20.8199	-1.1807	
	θ_c	-23.7042	-3.0926	
	TOTAL	0.3099	-1.9266	1.95

TABLE XI
SUMMARY OF OSCILLATORY BLADE LOADS (IN.-LB)
WITHOUT AND WITH VIBRATION COMPENSATION

Operating Condition	μ	Flapbending at 3.3 in.				Flapbending at 13.15 in.				Chordbending at 2.4 in.				Torsion at 9.28 in.			
		n = 2	n = 3	n = 4	n = 5	n = 2	n = 3	n = 4	n = 5	n = 2	n = 3	n = 4	n = 5	n = 2	n = 3	n = 4	n = 5
Without Oscillatory Control Input	0.191	30.1	4.4	1.6	3.5	16.0	1.9	3.0	4.3	21.0	2.2	8.3	19.4	1.2	0.7	0.4	0.6
	0.239	10.5	0.6	0.2	0.9	5.3	1.7	0.9	1.2	4.6	2.0	11.0	2.6	0.5	0.2	0.3	0.2
	0.443	16.4	2.7	0.1	1.6	9.2	3.2	0.4	3.5	9.4	1.7	10.5	7.7	0.9	0.6	0.3	0.2
	0.849	94.4	14.8	3.6	4.0	55.9	3.6	9.5	5.9	31.5	31.4	13.1	14.6	6.8	4.1	0.9	0.3
	0.851	18.9	8.6	1.5	3.1	17.7	4.6	3.4	5.8	17.4	10.9	18.9	10.7	3.3	2.4	0.7	0.4
With Oscillatory Control Input	0.191	29.6	1.1	2.9	0.4	16.1	4.4	5.0	3.0	19.2	22.7	10.9	3.9	1.0	1.2	0.4	4.5
	0.239	10.3	0.4	0.3	0.7	5.3	1.9	0.8	1.5	4.7	3.0	11.5	2.1	0.5	0.3	0.3	1.2
	0.443	12.3	1.3	1.3	1.1	7.5	2.7	0.5	1.3	7.7	3.5	13.6	8.7	0.8	1.4	1.4	1.7
	0.849	66.6	1.3	4.1	2.0	41.7	1.3	2.4	2.1	15.7	68.8	38.9	22.3	6.5	4.4	0.8	3.1
	0.851	20.2	2.4	6.5	4.1	16.5	3.8	7.0	2.5	17.5	13.6	75.6	7.0	2.3	4.0	0.7	3.5

The method of solution provides for intermode harmonic coupling through the 17th harmonic. This is accomplished by obtaining transient solutions of the 2-degree-of-freedom description of the rotor system described as constant coefficient linear differential equations over 10-degree sectors of the rotor azimuth.

The values of the coefficients for the system of differential equations evaluated in this work have been determined at the center of the sectors i. e., at 5°, 15°, 25°, etc.

The basis for the analytical formulation is founded on Shannon's sampling theorem which says that the discrete signal is equivalent to the continuous signal, provided that all frequency components of the latter are less than 1/2T cycles per second, T being the time between instants at which the signal is defined, (References 6 and 7). Since the solution also provides for a completely general transient solution, it can be used to calculate a Floquet solution by specializing the initial conditions. This has been done for the square spring oscillator case studied by M. A. Gockel and reported in the AHS Journal in January 1972. The problem statement which is exactly describable by this theoretical method was shown to yield the identical Floquet solutions as those reported. It is important to note that should the system be unstable, the harmonic balance method of solution would not directly reveal this instability.

Briefly, the initial conditions at the beginning of a sector are determined by calculating the terminal conditions for the previous sector which are then used to initialize the new sector. It has been found that essentially arbitrary conditions can be used to start the solution and that excellent steady-state conditions have been obtained for the conditions examined in six rotor revolutions. For each solution case presented, the rotor has been solved for eight revolutions to ensure that the second flapping mode contribution to the response has converged to a steady-state value accurate to at least four significant figures. The program is used to calculate closed-form analytic solutions over each 10-degree sector and therefore is not dependent on a particular method of numerical integration. (See Appendix A.) The method, however, when applied to the analysis of steady-state conditions, does require that sufficient solution time be calculated so that initial transients are dissippated to ensure that steady-state equilibrium is achieved (Reference 8).

The test configuration experimentally examined with respect to 1P flapbending distributions at μ = 0, including centerline measurements, has been compared with this analysis procedure on Figure 2, utilizing the two-mode description. This is a limited use of the analysis technique to establish test/analysis correlation. It is believed that the absence of time-dependent aerodynamics quasi-steady, largely accounts for the phase error in response. The centerline shaft moment measured was 0.75 of the calculated (a = 5.73). This may be due to the relatively low inflow of the test condition.

In general this correlation, including the spanwise distribution, appears reasonable.

The eigenvalues of each 10-degree sector are evaluated as part of the method. These are summarized in Tables XII, XIII, and XIV versus azimuth the μ = 0.191, 0.45, and 0.85 where the real and imaginary parts of the eigenvalues have been normalized by the noted natural-mode frequencies. The negative aerodynamic spring effects over azimuth $90 < \Psi < 270$ as well as the positive stiffening from $270 < \Psi < 90$ are as expected more pronounced on the first mode frequency. The effects of reduced aerodynamic spring and damping are also seen on the retreating side. These results show that both damping as well as frequency variations occur around the azimuth which influence the rotor response with harmonic excitations.

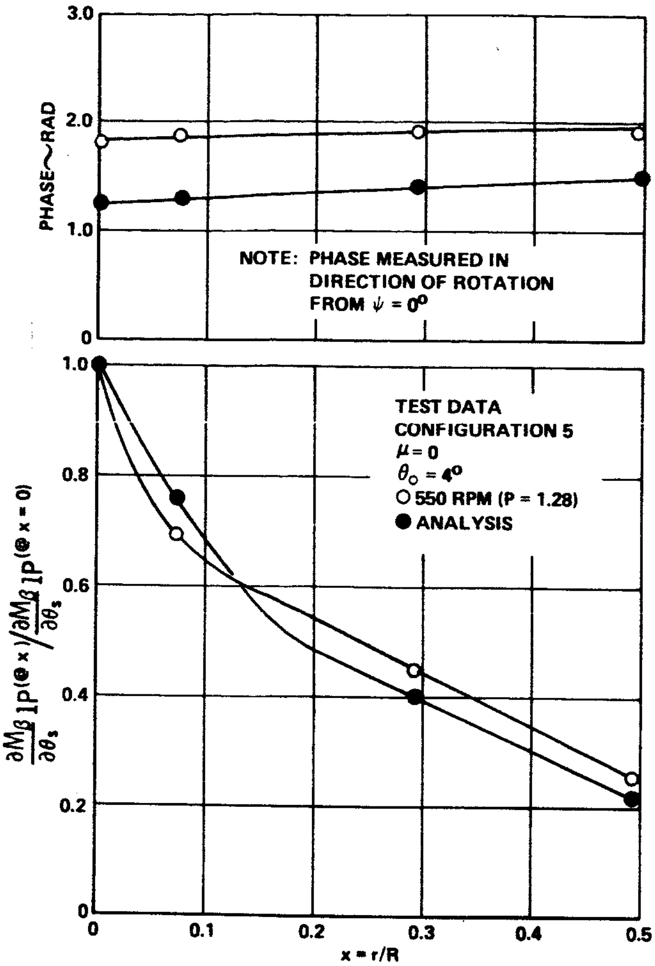

Figure 2. One-Per-Rev Blade Radial Flap-Bending Moment Distribution at $\mu = 0$.

The rotating frequencies and properties of the flapping modes noted in Tables XII, XIII, and XIV analytically describe the 7.5-ft-diameter rotor, configuration (5), 500-rotor-rpm condition for which all harmonic feathering tests were conducted. In an effort to further improve analytic correspondence with test data the slight change of the second flapping mode frequency resulted from matching collective blade angle selection at the test conditions. Details of the test model are given in References 9, 10 and 11.

The harmonic components of the blade root flap-bending moment (0P through 5P) were calculated for these advance ratios for unit perturbation of blade feathering angle at θ_{1c}, θ_{1s}, θ_{2c}, θ_{2s}, θ_{3c}, θ_{3s}, θ_{4c}, θ_{4s}, θ_{5c}, θ_{5s}, as well as for unit change in θ_0 and α

The single non-dimensional blade root, centerline flap-bending moment harmonic influence coefficients resulting from harmonic feathering are summarized in matrix form in Tables XV, XVI, and XVII for $\mu = 0.191, 0.45$, and 0.85. These are based on harmonic analysis of the moment at each condition for 36 equally spaced (10-degrees apart) azimuth intervals. Single-blade

TABLE XII
NORMALIZED EIGENVALUES* AT EACH 10-DEGREE AZIMUTHAL SECTOR FOR $\mu = 0.191$

		P = 1.34		P = 6.38	
SECTOR	Ψ^{o}	R_1	I_1	R_2	I_2
1	5	-.204	1.024	-.155	1.002
2	15	-.212	1.022	-.163	1.002
3	25	-.220	1.019	-.170	1.002
4	35	-.227	1.014	-.177	1.002
5	45	-.233	1.007	-.183	1.001
6	55	-.238	.999	-.187	1.001
7	65	-.242	.990	-.190	1.000
8	75	-.244	.980	-.192	1.000
9	85	-.245	.970	-.193	.999
10	95	-.244	.960	-.192	.998
11	105	-.242	.951	-.190	.998
12	115	-.239	.943	-.186	.997
13	125	-.234	.937	-.182	.997
14	135	-.228	.933	-.176	.997
15	145	-.221	.930	-.169	.996
16	155	-.213	.930	-.162	.996
17	165	-.205	.932	-.154	.996
18	175	-.197	.935	-.146	.997
19	185	-.188	.940	-.138	.997
20	195	-.180	.945	-.130	.997
21	205	-.172	.952	-.123	.997
22	215	-.165	.958	-.116	.998
23	225	-.159	.965	-.111	.998
24	235	-.154	.971	-.106	.998
25	245	-.150	.978	-.103	.999
26	255	-.148	.984	-.101	.999
27	265	-.147	.989	-.100	1.000
28	275	-.148	.995	-.101	1.000
29	285	-.150	.999	-.103	1.000
30	295	-.154	1.005	-.107	1.001
31	305	-.158	1.010	-.111	1.001
32	315	-.164	1.014	-.117	1.001
33	325	-.171	1.018	-.124	1.002
34	335	-.179	1.021	-.131	1.002
35	345	-.187	1.023	-.139	1.002
36	355	-.195	1.025	-.147	1.002

*SECTOR EIGENVALUES ARE GIVEN BY:

$$(R_1 + I_1\, i)\ (1.34\Omega)$$

AND $$(R_2 + I_2\, i)\ (6.38\Omega)$$

computed root flap-bending moment influence coefficients at $\mu = 0.45$ are compared with experimental 0.073R single-blade data, in parentheses, from Reference 1 and 12 in Table XVIII.

These appear reasonable when shear effects are considered.

It is important that the general character of these influence coefficients be established in future tests. These tests should be structured to permit measurement to confirm these distributions.

TABLE XIII
NORMALIZED EIGENVALUES* AT EACH 10-DEGREE AZIMUTHAL SECTOR FOR $\mu = .45$

		P = 1.34		P = 6.2	
SECTOR	Ψ^o	R_1	I_1	R_2	I_2
1	5	-.215	1.087	-.167	1.007
2	15	-.234	1.088	-.186	1.007
3	25	-.252	1.084	-.203	1.007
4	35	-.269	1.075	-.218	1.006
5	45	-.283	1.059	-.232	1.005
6	55	-.295	1.037	-.242	1.004
7	65	-.303	1.011	-.250	1.002
8	75	-.309	.982	-.255	1.000
9	85	-.311	.951	-.256	.998
10	95	-.310	.920	-.254	.996
11	105	-.305	.891	-.249	.995
12	115	-.297	.867	-.240	.993
13	125	-.285	.850	-.229	.992
14	135	-.271	.839	-.215	.991
15	145	-.255	.837	-.200	.991
16	155	-.237	.842	-.182	.991
17	165	-.218	.854	-.164	.992
18	175	-.197	.870	-.145	.992
19	185	-.177	.889	-.126	.993
20	195	-.158	.909	-.108	.994
21	205	-.139	.928	-.092	.995
22	215	-.123	.945	-.078	.996
23	225	-.109	.960	-.068	.997
24	235	-.098	.972	-.061	.998
25	245	-.089	.982	-.057	.998
26	255	-.085	.990	-.056	.999
27	265	-.083	.997	-.055	1.000
28	275	-.084	1.003	-.056	1.001
29	285	-.089	1.011	-.058	1.001
30	295	-.078	1.018	-.062	1.002
31	305	-.108	1.027	-.069	1.003
32	315	-.122	1.038	-.079	1.003
33	325	-.138	1.049	-.093	1.004
34	335	-.156	1.061	-.110	1.005
35	345	-.175	1.072	-.129	1.006
36	355	-.195	1.081	-.148	1.006

*SECTOR EIGENVALUES ARE GIVEN BY:

$(R_1 + I_1 i)\ (1.34\Omega)$

AND $(R_2 + I_2 i)\ (6.20\Omega)$

TABLE XIV
NORMALIZED EIGENVALUES* AT EACH 10-DEGREE AZIMUTHAL SECTOR FOR $\mu = .85$

		$P_1 = 1.34$		$P_2 = 6.20$	
SECTOR	Ψ^o	R_1	I_1	R_2	I_2
1	5	-.231	1.192	-.040	1.014
2	15	-.267	1.209	-.048	1.015
3	25	-.301	1.212	-.055	1.016
4	35	-.332	1.200	-.061	1.015
5	45	-.360	1.171	-.067	1.013
6	55	-.382	1.126	-.071	1.010
7	65	-.399	1.065	-.074	1.006
8	75	-.409	.992	-.076	1.002
9	85	-.413	.911	-.076	.997
10	95	-.411	.826	-.076	.992
11	105	-.402	.745	-.073	.988
12	115	-.387	.675	-.070	.984
13	125	-.366	.625	-.065	.982
14	135	-.339	.603	-.060	.980
15	145	-.308	.611	-.053	.980
16	155	-.274	.645	-.040	.981
17	165	-.237	.698	-.039	.983
18	175	-.199	.759	-.031	.986
19	185	-.160	.822	-.023	.989
20	195	-.123	.879	-.016	.992
21	205	-.090	.925	-.012	.993
22	215	-.062	.954	-.011	.994
23	225	-.043	.970	-.012	.996
24	235	-.034	.977	-.014	.997
25	245	-.032	.983	-.015	.998
26	255	-.032	.990	-.015	.999
27	265	-.033	1.000	-.016	1.000
28	275	-.032	1.009	-.015	1.000
29	285	-.032	1.016	-.015	1.001
30	295	-.034	1.021	-.014	1.002
31	305	-.043	1.028	-.012	1.004
32	315	-.061	1.040	-.011	1.006
33	325	-.088	1.063	-.013	1.007
34	335	-.120	1.094	-.017	1.008
35	345	-.156	1.130	-.024	1.010
36	355	-.193	1.165	-.032	1.012

*SECTOR EIGENVALUES ARE GIVEN BY:

$(R_1 \pm I_1 i)\ (1.34\Omega)$

AND $(R_2 \pm I_2\Omega)\ (6.20\Omega)$

TABLE XV

$\frac{C_{RM}}{a\sigma}$ – BLADE ROOT (STA 0) BENDING MOMENT INFLUENCE COEFFICIENT MATRIX FOR μ = 0.191
(P_1 = 1.34, P_2 = 6.38)

	C_{β_0}	$C_{\beta_{1C}}$	$C_{\beta_{1S}}$	$C_{\beta_{2C}}$	$C_{\beta_{2S}}$	$C_{\beta_{3C}}$	$C_{\beta_{3S}}$	$C_{\beta_{4C}}$	$C_{\beta_{4S}}$	$C_{\beta_{5C}}$	$C_{\beta_{5S}}$
$\Delta\alpha$	.0034	.0009	-.0016	-.0001	-.0001	0	0	0	0	0	0
$\Delta\theta$	.0132	.0049	-.0111	-.0007	-.0005	-.0001	0	0	0	0	0
$\Delta\theta 1S$	.0036	.0057	-.0225	-.0018	-.0003	0	.0002	0	0	0	0
$\Delta\theta 1C$	-.0005	-.0213	-.0045	-.0001	.0018	.0002	0	0	0	0	0
$\Delta\theta 2S$	0	-.0056	-.0004	.0018	.0031	.0014	-.0009	.0002	.0003	0	0
$\Delta\theta 2C$	-.0003	-.0005	.0057	.0031	-.0018	-.0009	-.0014	.0003	-.0002	0	0
$\Delta\theta 3S$	0	-.0001	.0004	.0001	.0002	-.0046	-.0012	.0015	-.0014	.0001	.0003
$\Delta\theta 3C$	0	.0004	0	.0002	-.0001	-.0012	.0046	-.0014	-.0015	.0003	-.0001
$\Delta\theta 4S$	0	0	0	0	.0001	-.0010	.0017	-.0076	-.0026	.0017	-.0020
$\Delta\theta 4C$	0	0	0	.0001	-.0001	.0017	.0009	-.0026	.0076	-.0020	-.0017
$\Delta\theta 5S$	.0119	0	0	0	0	.0002	.0002	-.0015	.0024	-.0101	-.0033
$\Delta\theta 5C$	0	0	0	0	0	.0002	-.0002	.0024	.0015	-.0033	.0101

TABLE XVI

$\frac{C_{RM}}{a\sigma}$ – BLADE ROOT (STA 0) BENDING MOMENT INFLUENCE COEFFICIENT MATRIX FOR μ =.45
(P_1 = 1.34, P_2 = 6.20)

	C_{β_0}	$C_{\beta_{1C}}$	$C_{\beta_{1S}}$	$C_{\beta_{2C}}$	$C_{\beta_{2S}}$	$C_{\beta_{3C}}$	$C_{\beta_{3S}}$	$C_{\beta_{4C}}$	$C_{\beta_{4S}}$	$C_{\beta_{5C}}$	$C_{\beta_{5S}}$
$\Delta\alpha$	.0085	.0053	-.0089	-.0010	-.0012	-.0004	-.0004	-.0001	-.0001	0	0
$\Delta\theta$	.0160	.0135	-.0276	-.0038	-.0029	-.0009	-.0004	-.0001	-.0002	0	0
$\Delta\theta 1S$	.0087	.0102	-.0292	-.0048	-.0016	-.0004	.0007	-.0006	0	0	0
$\Delta\theta 1C$	-.0011	-.0226	-.0034	-.0004	.0046	.0011	.0002	.0001	.0003	0	0
$\Delta\theta 2S$	0	-.0130	-.0006	.0006	.0046	.0036	-.0020	.0009	.0015	-.0002	.0002
$\Delta\theta 2C$	-.0015	-.0024	.0142	.0043	.0001	-.0020	-.0035	.0015	-.0009	.0001	.0002
$\Delta\theta 3S$	0	0	.0023	.0004	.0010	-.0057	-.0032	.0038	-.0036	.0008	.0016
$\Delta\theta 3C$	-.0002	.0022	-.0002	.0007	-.0001	-.0033	.0057	-.0036	-.0038	.0016	-.0008
$\Delta\theta 4S$	0	-.0001	0	.0003	.0007	-.0026	.0042	-.0090	-.0046	.0043	-.0048
$\Delta\theta 4C$	0	0	0	.0004	0	.0042	.0026	-.0046	.0090	-.0048	-.0043
$\Delta\theta 5S$	0	0	0	0	.0003	.0008	.0008	-.0038	.0058	-.0118	-.0055
$\Delta\theta 5C$	0	0	0	0	.0003	.0008	-.0009	.0058	.0038	-.0054	.0118

TABLE XVII

$\frac{C_{RM}}{a\sigma}$ – BLADE ROOT (STA 0) BENDING MOMENT INFLUENCE COEFFICIENT MATRIX FOR μ = .85
(P_1 = 1.34, P_2 = 6.20)

	C_{β_0}	$C_{\beta_{1C}}$	$C_{\beta_{1S}}$	$C_{\beta_{2C}}$	$C_{\beta_{2S}}$	$C_{\beta_{3C}}$	$C_{\beta_{3S}}$	$C_{\beta_{4C}}$	$C_{\beta_{4S}}$	$C_{\beta_{5C}}$	$C_{\beta_{5S}}$
$\Delta\alpha$	.0201	.0227	-.0296	-.0056	-.0102	-.0037	-.0039	0	-.0021	0	-.0015
$\Delta\theta$	.0253	.0378	-.0598	-.0141	-.0155	-.0061	-.0039	0	-.0032	-.0003	-.0018
$\Delta\theta 1S$	.0192	.0278	-.0490	-.0117	-.0114	-.0036	-.0004	-.0019	-.0014	-.0005	-.0001
$\Delta\theta 1C$	-.0024	-.0258	-.0015	-.0012	.0085	.0035	.0008	.0003	.0022	0	.0009
$\Delta\theta 2S$	-.0006	-.0229	-.0007	-.0026	.0079	.0081	-.0034	.0024	.0054	-.0019	.0016
$\Delta\theta 2C$	-.0056	-.0110	.0308	.0084	.0067	-.0026	-.0064	.0052	-.0019	.0013	.0023
$\Delta\theta 3S$	-.0003	-.0014	.0076	.0010	.0035	-.0088	-.0082	.0100	-.0084	.0033	.0049
$\Delta\theta 3C$	-.0009	.0060	0	.0029	-.0009	-.0084	.0089	-.0084	-.0100	.0048	-.0033
$\Delta\theta 4S$	-.0005	-.0004	.0003	.0013	.0008	-.0067	.0087	-.0135	-.0100	.0112	-.0100
$\Delta\theta 4C$	-.0004	.0002	-.0002	.0007	-.0014	.0087	.0067	-.0100	.0134	-.0101	-.0112
$\Delta\theta 5S$	0	.0001	.0006	.0002	-.0003	.0029	.0023	-.0088	.0124	-.0167	-.0115
$\Delta\theta 5C$	0	.0006	-.0002	-.0003	-.0002	.0023	-.0029	.0124	.0088	-.0116	.0167

TABLE XVIII
BLADE ROOT (STA 0) BENDING MOMENT (IN-LB)/DEG INFLUENCE MATRIX FOR μ = .45
(Ω= 52.36, P_1 = 1.34, P_2 = 6.20)

	β_0	β_{1C}	β_{1S}	β_{2C}	β_{2S}	β_{3C}	β_{3S}	β_{4C}	β_{4S}	β_{5C}	β_{5S}	LIFT
$\Delta\alpha$	19	12	-20	-2	-3	-1 (1)	-1 (-2)	0	0	0 (1)	0 (-1)	6
$\Delta\theta$	36	31	-62	-9	-7	-2 (1)	-1 (1)	0	0	0 (1)	0 (0)	10
$\Delta\theta 1S$	20	23	-66	-11	-4	-1 (1)	2 (-2)	-1	0	0 (1)	0 (0)	6
$\Delta\theta 1C$	-2	-51	-8	-1	10	3 (0)	0 (1)	0	1	0 (0)	0 (0)	0
$\Delta\theta 2S$	0	-29	-1	1	10	8	-5	2	3	-1	0	0
$\Delta\theta 2C$	-3	-5	32	10	0	-5	-8	3	-2	0	0	-1
$\Delta\theta 3S$	0	0	5	1	2	-13	-7	9	-8	2	4	0
$\Delta\theta 3C$	0	5	-1	2	0	-7	13	-8	-9	4	-2	0
$\Delta\theta 4S$	0	0	0	1	2	-6 (0)	9 (6)	-20 (-8)	-10 (-5)	10 (-5)	-11 (-1)	0
$\Delta\theta 4C$	0	0	0	1	0	9 (6)	6 (-2)	10 (-4)	20 (7)	-11 (-6)	-10 (3)	0
$\Delta\theta 5S$	0	0	0	0	1	2	2	-9	13	-27	-12	0
$\Delta\theta 5C$	0	0	0	0	1	2	-2	13	9	-12	27	0

Full-Scale Control Loads

The feasibility of active vibration attenuation depends on the capability of the rotor to generate cancelling shaft moments and shears while control forces and displacements remain within acceptable limits.

Since full-scale data are the most relevant from the standpoint of hardware test background, the CL 840/AMCS (Advanced Mechanical Control System) Cheyenne rotor configuration, at a gross weight of 20,000 and with a rotor shaft moment of 100,000 in.-lb, was analyzed for hovering flight to gain a numerical measure of how loads compare with limits. In this analysis three higher harmonic blade-feathering excitations, 3P, 4P and 5P, were examined to determine the relationships among control loads, shaft moments and shear forces. The Lockheed Rotor Blade Loads Prediction Model was used for this analysis; 68 finite elements were used to describe the system. The calculated results, based on 1-degree excitation levels, are summarized in Table XIX.

TABLE XIX
CL 840 ANALYSIS - SHAFT AND BLADE LOADS DUE TO ONE-DEGREE OF HIGHER HARMONIC BLADE-FEATHERING MOTIONS

	FEATHERING FREQUENCY						
	3φ		4φ		5φ		Endurance
	Amplitude	Phase	Amplitude	Phase	Amplitude	Phase	Limit, in.-lb
Shaft Forces							
4P H-force	380 lb	61°	40 lb	59°	310 lb	34°	
4P Y-force	380 lb	84°	40 lb	83°	310 lb	12°	
4P Pitching Moment	22,000 in.-lb	83°	0		108,000 in.-lb	8°	325,000
4P Rolling Moment	22,000 in.-lb	16°	0		108,000 in.-lb	76°	
4P Thrust	0		3000 lb	40°	0		
Blade Root Torsion * Harmonic							
Steady	-3800 in.-lb		-4000 in.-lb		-3900 in.-lb		
1P	210 in.-lb	11°	210 in.-lb	11°	220 in.-lb	11°	
2P	80 in.-lb	49°	50 in.-lb	42°	50 in.-lb	39°	15,500
3P	1500 in.-lb	15°	70 in.-lb	82°	40 in.-lb	84°	
4P	130 in.-lb	47°	13,300 in.-lb	88°	400 in.-lb	57°	
5P	20 in.-lb	27°	80 in.-lb	35°	7800 in.-lb	10°	

* Pitch link forces are internal loads between the blade and swashplate and therefore self-cancelling.

The calculated root torsion moments shown in the table reflect both the feathering moments at the primary exciting frequency and the interharmonic coupling terms; as expected, the latter are considerably less. Pitch link loads can be determined by multiplying the root torsion moment by 0.1 (to account for all applicable geometry); endurance limit of the pitch link load is 1550 pounds.

The 7.5-foot hingeless rotor model data showed that 0.2 to 0.6-degree cyclic angle excitation levels were required. Study of CL 840 test data indicates that similar blade excitation would be expected with a full-scale, four-bladed rotor. The CL 840 data are not yet published in documents that can be referenced, however, this material is expected to be published during 1974.

In summary, full-scale data founded on endurance limit considerations indicate that internal blade loads and control loads will not limit the trim flight use of periodic variation of conventional controls for vibration attenuation.

Conclusions

The present report is a preliminary evaluation of the concept of vibration reduction by properly selected oscillatory collective and cyclic control applications. The investigations are based on experimental frequency response data covering advance ratios from approximately 0.2 to 0.85.

Because there was no instrumentation for the measurement of the pitch and roll vibrations, these values were obtained by properly adding up the flap-bending moments at 3.3 inches. Any other quantity representing pitch/roll vibrations can be compensated for in the same fashion.

The calculated control inputs required for vibration reduction stay within acceptable limits. For four of the five conditions tested they are smaller than the values used for the frequency response tests. The blade pitch variations required for vibration alleviation vary, depending on the advance ratio, less than 1° for $.2 \leqslant \mu \leqslant .45$ and $\sim 3^{\circ}$ for $\mu = .85$.

As to be expected, the compensating controls greatly affect the blade loads, i.e., torsion, flap- and chordwise bending. With regard to flap-bending at 3.3 inches (root flexure), the following statements can be made:

- 3 and 5P flap moments were, by command, drastically reduced
- 2P flap moments were least affected. These were the largest oscillatory loads.
- 4P flap moment increments generally increased with increasing advance ratio, but were small relative to the 2P flap moments.

As a general rule, chordwise bending and blade torsion increments also increase with the advance ratio. At lower μ values the loads are not critical. It is concluded that the concept investigated is primarily suited for low and medium advance ratios, i.e., for the speed-range of present day rotary wing aircraft. The latter application appears promising and further studies and tests are suggested. Instrumentation to determine rotor vertical and inplane shear forces should be incorporated in such future tests. Also a system with a first inplane frequency in the vicinity of 1.5P in combination with a flapping frequency of 1.1P should be tested at conventional advance ratios to provide experimental data representative of current designs.

References

1. London, R. J., Watts, G. A., and Sissingh, G. J., EXPERIMENTAL HINGELESS ROTOR CHARACTERISTICS AT LOW ADVANCE RATIO, NASA CR-1148A, December 1973.

2. USAAVLABS Technical Report 69-39, SUPPRESSION OF TRANSMITTED HARMONIC VERTICAL AND INPLANE ROTOR LOADS BY BLADE PITCH CONTROL, Balcerak, J. C., and Erickson, J. C., Jr., Ft Eustis, Virginia, July 1969.

3. ASRL - Technical Reference 150-1, HIGHER HARMONIC BLADE PITCH CONTROL FOR HELICOPTER, Shaw, John Jr., Massachusetts, December 1968.

4. USAAVLABS Technical Reference 70-58, WIND TUNNEL INVESTIGATION OF A QUARTER-SCALE TWO-BLADED HIGH-PERFORMANCE ROTOR IN A FREON ATMOSPHERE, Lee, Charles; Charles, Bruce, and Kidd, David, Ft Eustis, Virginia, February 1971.

5. Sissingh, G. J., DYNAMICS OF ROTORS OPERATING AT HIGH ADVANCE RATIOS J. American Helicopter Society, 13(3) July 1968.

6. C. E. Shannon, COMMUNICATION IN THE PRESENCE OF NOISE, Proc. IRE, Vol. 37, January 1949, p.11.

7. DeRusso, P. M., Roy, R. J., and Close, C. M., STATE VARIABLES FOR ENGINEERS, New York, John Wiley and Sons, Inc. 1967, p. 6-9.

8. Donham, R. E., Subsection titled "RESPONSE OF HELICOPTER ROTOR BLADES TO GUST ENVIRONMENTS" in NUCLEAR HARDENING SURVIVABILITY DESIGN GUIDE FOR ARMY AIRCRAFT. This report is being prepared by the B-1 Division of Rockwell International under Army Contract DAAJ02-73-C-0032.

9. Kuczynski, W. A., Sissingh, G. J., RESEARCH PROGRAM TO DETERMINE ROTOR RESPONSE CHARACTERISTICS AT HIGH ADVANCE RATIOS, LR 24122, February 1971, prepared under Contract NAS 2-5419 for U. S. Army Air Mobility Research and Development Laboratory, Ames Directorate, Moffet Field, California.

10. Kuczynski, W. A., Sissingh, G. J., CHARACTERISTICS OF HINGELESS ROTORS WITH HUB MOMENT FEEDBACK CONTROLS INCLUDING EXPERIMENTAL ROTOR FREQUENCY RESPONSE, LR 25048, January 1972, prepared under Contract NAS 2-5419 for U. S. Army Air Mobility Research and Development Laboratory, Ames Directorate, Moffet Field, California. (Volumes I and II).

11. Kuczynski, W. A., EXPERIMENTAL HINGELESS ROTOR CHARACTERISTICS AT FULL SCALE FIRST FLAP MODE FREQUENCIES LR 25491, October 1972, prepared under Contract NAS 2-5419 for U. S. Army Air Mobility Research and Development Laboratory, Ames Directorate, Moffet Field, California.

12. Watts, G. A. and London, R. J., VIBRATION AND LOADS IN HINGELESS ROTORS, Vol. I and II, NASA CR-114562, September 1972.

Appendix A

The transient response solution of a system described by constant coefficient linear differential equations is developed in this appendix. The single-degree-of-freedom case with arbitrary initial conditions and solution of the general case for an nth order system with both zero and nonzero initial conditions is reported.

Given the single degree of freedom:

$$A \frac{d^2\beta}{dt^2} + B \frac{d\beta}{dt} + C\beta = F(t) \tag{1}$$

where A, B, and C are constants, then

$$A\mathcal{L}\left(\frac{d^2\beta}{dt^2}\right) + B\mathcal{L}\left(\frac{d\beta}{dt}\right) + C\mathcal{L}(\beta) = \mathcal{L}(F(t))$$

where $\mathcal{L}$ is the Laplace transform operator. This yields

$$(As^2 + Bs + C)\ \beta(s) = F(s) + \beta(0)(As + B) + \dot{\beta}(0)A \tag{2}$$

or

$$\beta(s) = \frac{F(s) + \beta(0)(As + B) + \dot{\beta}(0)A}{As^2 + Bs + C}$$

If a positive constant step load of magnitude + L is the form of F(t), then

$$\mathcal{L}(F(t)) = F(s) = \frac{+L}{s}$$

and

$$\beta(s) = \frac{L}{A(s)(s-\alpha)(s-\gamma)} + \frac{\beta(0)As}{A(s-\alpha)(s-\gamma)} + \frac{\beta(0)B + \dot{\beta}(0)A}{A(s-\alpha)(s-\gamma)} \tag{3}$$

Where $\beta(0)$ and $\dot{\beta}(0)$ are the values of the variable β at time $t = 0$ and α, γ are the roots of $s^2 + Bs/A + C/A$, $\beta(s)$ transformed back into the time plane is accomplished through use of the inverse Laplace transform of the form $\frac{P(s)}{Q(s)}$

where
$P(s)$ = polynomial of degree less than n

and
$Q(s) = (s-\alpha_1)(s-\alpha_2)\ldots(s-\alpha_n)$

where $\alpha_1, \alpha_2, \ldots \alpha_n$ are all distinct, this yields

$$\beta(t) = \sum_{k=1}^{n} \frac{P(\alpha_k)}{Q'(\alpha_k)} e^{\alpha_k t} \tag{4}$$

In the case cited

$$Q(s) = A(s)(s-\alpha)(s-\gamma)$$

where

$$\alpha_1 = 0$$

$$\alpha_2 = \alpha$$

$$\alpha_3 = \gamma$$

and

$$P(s) = L + \left[\beta(0)A\right] s^2 + \left[\beta(0)B + \dot{\beta}(0)A\right] s$$

Therefore

$$\beta(t) = \sum_{k=1}^{n} \frac{P(\alpha_k)}{Q'(\alpha_k)} e^{\alpha_k t}$$

$$\beta(t) = \frac{L}{A(-\alpha)(-\gamma)} + \left[\frac{L + [\beta(0)A]\alpha^2 + [\beta(0)B + \dot{\beta}(0)A]\alpha}{A(+\alpha)(+\alpha-\gamma)}\right] e^{\alpha t} + \left[\frac{L + [\beta(0)A]\gamma^2 + [\beta(0)B + \dot{\beta}(0)A]\gamma}{(A)(+\gamma)(\gamma-\alpha)}\right] e^{\gamma t} \tag{5}$$

Extension to the general case is accomplished as follows. Given the general determinantal equation:

$$\left\{s^2\left[A\right] + s\left[B\right] + \left[C\right]\right\}\left\{\beta(s)\right\} = \left\{F(s)\right\} \tag{6}$$

Where the elements of matrix A, B, and C are constants, using Cramer's Rule:

$$\beta_i(s) = \frac{\left|\begin{matrix}\text{Denominator with} \\ \text{Column i replaced by} \quad F(s)\end{matrix}\right|}{\left| s^2\left[A\right] + s\left[B\right] + \left[C\right] \right|} \tag{7}$$

Expanding

$$\left| s^2\left[A\right] + s\left[B\right] + \left[C\right] \right|$$

yields

$$A_o(s-\alpha_1)(s-\alpha_2)\ \ldots\ (s-\alpha_n) \tag{8}$$

where

A_o = Coefficient of highest power term

α_i $(i = 1 \ldots n)$ are the eigen values (roots) of the determinantal equation

Case 1 - Zero Initial Conditions

Assume $\beta_i(0)$ and $\dot{\beta}_i(0)$ for all i are both zero and that a positive unit load acts on β_e and that the response of β_f is to be determined. Then

$$\left\{F(s)\right\} = \left\{\begin{matrix}+ 1/s \text{ in row e with all other} \\ \text{rows equal } \underline{0}\end{matrix}\right\}$$

Defining

$$\left| s^2[A] + s[B] + [C] \right|_{(e,f)} \tag{9}$$

as the original determinantal equation with Row e and Column f removed and all the remaining rows and columns moved up and to the left, respectively, this forms a determinantal equation of one less order.

Based on the earlier development in the s-plane

$$\mathcal{L}\left(\beta_f(t)\right) = \frac{a_o}{s} + \frac{a_1}{s-\alpha_1} + \frac{a_2}{s-\alpha_2} + \ldots + \frac{a_n}{s-\alpha_n}$$

and in the time plane

$$\beta_f(t) = a_o + a_1 e^{\alpha_1 t} + a_2 e^{\alpha_2 t} + \ldots + a_n e^{\alpha_n t} \tag{10}$$

where

$$a_o = \frac{(-1)^{(e+f)} D(o)_{e,f}}{A_o \prod_{i=1}^{n} \alpha_i}$$

and

$$a_j = \frac{(-1)^{(e+f)} D(\alpha_j)_{e,f}}{\alpha_j A_o \prod_{i=1}^{n} (\alpha_j - \alpha_i)} \qquad i \neq j$$

A_o is determined by the relationship

$$D(o) = A_o \prod_{i=1}^{n} \alpha_i$$

$D(o)_{e,f}$ and $D(\alpha_j)_{e,f}$ are formed from the original determinantal equation with Row e and Column f removed and all the remaining rows and columns moved up and to the left, respectively, evaluated at o and α_j. The α_j are the roots of the original determinantal equation before Row e and Column f were removed. These roots are assumed distinct, an unimportant limitation for most physical systems. Note that this solution does not preclude instability either aperiodic or oscillatory.

In practice the eigenvalues are obtained prior to the formation of the coefficients and are examined to verify the distinct character of the eigenvalues.

Scalar multiplication of this solution provides the result for the nonunit loading case. Summation of solutions obtained for loadings at each coordinate can be used to provide the general solution for this case where $\beta_i(0)$ and $\dot{\beta}_i(0)$ for all i are both zero, i.e., that the initial conditions at time zero are all zero.

In most applications the restriction that the initial conditions are zero is an unacceptable constraint and this condition has been relaxed; the solution follows.

Case 2 - Nonzero Initial Conditions

The general form of F(s) now becomes:

$$\left\{F(s)\right\} = \left\{\frac{L_i}{s}\right\} + \left\{ s[A] + [B]\right\}\left\{\beta_i(0)\right\} + \left\{[A]\left\{\dot{\beta}_i(0)\right\}\right\} \tag{11}$$

where L_i are the forces applied at each coordinate β_i and $\beta_i(0)$ and $\dot{\beta}_i(0)$ are the positions and rates of the coordinates at time zero (initiations of the solution). In this case place the column $s\left\{F(s)\right\}$ into the column location of the coordinate for which the response is desired without reduction of the order. Then

$$P(s) = \left| \begin{array}{c} \text{Column i} \\ \downarrow \\ s\left\{F(s)\right\} \end{array} \right| \tag{12}$$

where all other terms are

$$\left| s^2[A] + s[B] + [C] \right|$$

and

$$Q(S) = A_0(s-\alpha_0)(s-\alpha_1)\ldots(s-\alpha_n) \tag{13}$$

where the α's are the eigenvalues of the determinantal equation

$$\left\{ s \left| s^2[A] + s[B] + [C] \right| \right\} = 0$$

Then

$$\beta_i(t) = \sum_{k=0}^{n} \frac{P(\alpha_k)}{Q'(\alpha_k)} e^{\alpha_k t} \tag{14}$$

where s = 0 and the remaining eigenvalues of the general determinantal equation form the set of α_k's, and A_0 is determined by the relationship

$$D(0) = A_0 \prod_{i=1}^{n} \alpha_i \tag{15}$$

as given in Case 1.